Evaluation of bridge-function diagrams via Mayer-sampling Monte Carlo simulation

Sang Kyu Kwak and David A. Kofke
Department of Chemical and Biological Engineering, University at Buffalo, The State University of New York, Buffalo, New York 14260-4200

(Received 13 December 2004; accepted 30 December 2004; published online 11 March 2005)

We report coefficients of the *h*-bond expansion of the bridge function of the hard-sphere system up to order ρ^4 (where ρ is the density in units of the hard-sphere diameter), which in the highest-order term includes 88 cluster diagrams with bonds representing the total correlation function $h(r)$. Calculations are performed using the recently introduced Mayer-sampling method for evaluation of cluster integrals, and an iterative scheme is applied in which the $h(r)$ used in the cluster integrals is determined by solution of the Ornstein–Zernike equation with a closure given by the calculated clusters. Calculations are performed for reduced densities from 0.1 to 0.9 in increments of 0.1. Comparison with molecular simulation data shows that the convergence is very slow for the density expansion of the bridge function calculated this way. © *2005 American Institute of Physics*.
[DOI: 10.1063/1.1860559]

I. INTRODUCTION

Integral equation theory[1,2] (IET) provides a means to predict the behavior of condensed phases from the intermolecular interactions. IET methods are useful because they are computationally efficient, and in some cases can yield completely to analytic treatment. A primary aim in these approaches is the direct evaluation of the pair correlation function $g(r)$, where r is the relative distance of a pair of molecules (which we take here as monatomic). Theories can be developed in terms of the direct correlation function $c(r)$, which is defined by the Ornstein–Zernike (OZ) equation,

$$h(r) = c(r) + \rho \int c(r')h(|r - r'|)dr', \tag{1}$$

where $h(r)=g(r)-1$ and ρ is the number density of molecules. Application of Eq. (1) requires a closure, which also introduces into the theory the pair potential $u(r)$ that defines the molecular interactions. The basic idea is to solve another relation between $c(r)$ and $h(r)$ with the OZ equation. A particularly suitable choice involves the cavity distribution function $y(r)$,

$$y(r) \equiv g(r)\exp[\beta u(r)] = \exp[h(r) - c(r) + b(r)], \tag{2}$$

where $\beta=1/k_BT$, k_B is Boltzmann's constant, and T is the temperature. This relation does not yet provide a closure, because it introduces another quantity $b(r)$, which is known as the bridge function. From this point approximations are introduced that yield a well defined set of integral equations that can yield $g(r)$ from $u(r)$. The hypernetted chain (HNC) closure simply takes $b(r)=0$, while the Percus–Yevick (PY) closure goes one step further and takes also $y(r)=1+h(r)-c(r)$; the PY approximation seems to benefit from a cancellation of errors when applied to short-ranged potentials. The approximate nature of both of these closures is evident in several ways. When applied to the hard-sphere (HS) model, they yield pressures (via the virial) that are too high (HNC) and too low (PY) in comparison to molecular simulation. They also can be shown to lead to certain thermodynamic inconsistencies, and methods to improve these approaches use similar approximations, but proceed in different ways that remove the inconsistencies.[3–10]

Several of the approaches to improve IET closures focus on the neglected bridge function $b(r)$. There are two main routes to construct $b(r)$. One general approach works within the IET framework, deriving $b(r)$ from measurements or approximations. The former then is an empirical approach: molecular simulation is used to obtain accurate $g(r)$ from which $b(r)$ is evaluated via its definition.[11] The resulting form is sometimes fitted to give an empirical expression through adjustable parameters.[12–14] The parametrization processes have been shown to provide fast and reliable ways to construct $b(r)$ for some interesting model systems. However, this approach sometimes shows inaccuracy with respect to the signs of $b(r)$[9,15,16] and zero-separation theorems.[17–21] Approaches based more on first principles include a perturbation method, which approximates $b(r)$ of the potential of interest using a simpler short-ranged potential.[22–25]

Another route to obtain $b(r)$ is a direct evaluation in terms of the bridge-function coefficients defined by the density expansion of the function

$$b(r) = \sum_{n=2}^{\infty} b_n(r)\rho^n. \tag{3}$$

The coefficients $b_n(r)$ are multidimensional integrals which can be written in terms of cluster diagrams,[1,26] which consist of n field (black) points, two reference (white) points in relative distance r, and bonds that define the integrand. In one treatment the bonds represent the Mayer function $f(r) \equiv \exp[-\beta u(r)]-1$, while in another the bonds represent the total correlation function $h(r)$. An advantage of the f-bond expansion is that the coefficients $b_n(r)$ remain truly density independent. In comparison, because $h(r)$ depends on den-

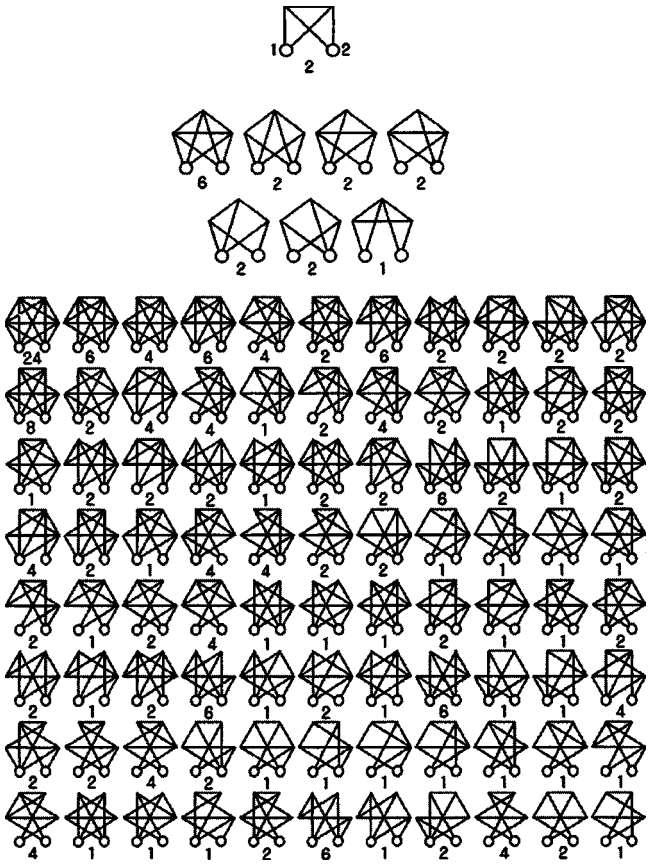

FIG. 1. Clusters in the *h*-bond density expansion of the bridge function [Eq. (3)]. The first row shows the single diagram in b_2. The numbers 1 and 2 label the root points (for clarity, these labels are omitted in the other diagrams). The second and third rows show diagrams in b_3, which consists of seven distinct clusters. The remainder of the rows show diagrams in b_4, which consists of 88 distinct clusters. Values of each coefficient can be obtained from evaluating the sum of all diagrams, respectively. Numbers below diagrams represent their symmetry numbers; the weight of each diagram is the reciprocal of the given value.

sity, coefficients given in terms of it implicitly incorporate higher-order components of the density expansion, and they must be evaluated separately at each density. This is also the advantage of the *h*-bond expansion. One might expect fewer terms in the expansion to yield a better representation of $b(r)$, because the higher-order terms are present implicitly.

Stell has given a prescription to construct bridge diagrams composed of *h* bonds.[26] For instance, the second, third, and fourth coefficients, b_2, b_3, and b_4 are shown in Fig. 1. It is worth noting that the number of diagrams in b_3 could be further reduced to 5 and those in b_4 to 56 because some of diagrams are symmetric with respect to exchange of the labels of the white reference points, and thus have identical values.

Evaluating the bridge-function coefficients is a difficult task because (1) their number expands rapidly with increasing order of the expansion and (2) each cluster diagram represents a high-dimensional integral over the coordinates of several particles. Nijboer and van Hove[27] derived an analytical solution of b_2 with *f* bonds for the hard-sphere system, and b_3 diagrams for hard spheres in the *f*-bond series were numerically calculated by Ree and co-workers.[28] Both coefficients were also calculated by Attard and Patey[29] for hard-sphere systems and their mixtures using a Legendre polynomial expansion, and they used these results to form a Padé approximant that represented the function well to higher densities and for highly asymmetric mixtures. There have been several recent attempts to perform these calculations to higher orders and for other models. Perkyns, Dyer, and Pettitt[30] applied the Attard–Patey formalism to calculate b_2 and b_3 for the *h*-bond expansion for the Lennard–Jones (LJ) system. They obtained a self-consistent solution through iteration, in which the calculated bridge-function coefficients are used to estimate $b(r)$ and then $h(r)$, which is in turn used to calculate the bridge-function coefficients. We apply this iterative approach in the present work, but employ a different method for calculating the relevant cluster integrals.

Rast, Fries, and Krienke[16] first proposed a general biased Monte Carlo (MC) method for evaluation of cluster integrals, and used it to calculate b_2 and b_3 for the *h*-bond expansion for the HS and LJ systems; in their work they used accurate data for $h(r)$ from the literature to calculate the coefficients. The form of the bias was obtained in part by a variance minimization procedure, supplemented by application of some judgment regarding the appropriate form to use for large separations, including a finite volume to contain the particles. The bias significantly improved the MC sampling. Labík *et al.*[31] built on the ideas of Rast *et al.* and evaluated up to b_5 for the *f*-bond expansion applied to the hard-sphere model. Unlike the approach of Rast *et al.*, Labík *et al.* evaluated the cluster integrals separately (or in small groups) in different MC samples, rather than together as their sum for b_n. For each cluster, they identified a *framework* cluster, which was chosen for its analytic tractability and for its similarity to the cluster(s) of interest. The framework cluster provided the probability distribution for the biased MC sampling. The quantity averaged in their method is the ratio of the desired cluster to the framework cluster.

Recently, Singh and Kofke[32] recognized that molecular simulation methods developed for evaluation of the free energy could be applied toward the evaluation of cluster integrals. They proposed the term *Mayer sampling* to describe this general approach and application. In the present work we apply the Mayer-sampling method to evaluate up to the fourth coefficient of the *h*-bond expansion of $b(r)$, applied to the hard-sphere fluid system.

In Sec. II, we describe the Mayer-sampling technique and briefly explain the procedure used to solve Eqs. (1) and (2) with respect to $b(r)$. In Sec. III, we describe computational details and in Sec. IV we present and discuss our results. In the last section, we summarize and conclude.

II. BACKGROUND

The thermodynamic free energy is known from statistical mechanics to be directly related to the partition function, for classical fluids is a straightforward configurational integral. Thus methods to evaluate free energies are methods for evaluation of configurational integrals, and if cast in the proper form, these methods can be applied to calculate the configurational integrals arising in cluster expansion. Thus we might expect that the rich array of methods developed for

free-energy calculations should be adaptable to this problem. We consider here specifically applications to diagrams containing two root points with no external fields, but the formulas are easily generalized.

The most straightforward free-energy method is free-energy perturbation, which is based upon this relation,

$$\Gamma(r) = \Gamma_o \langle \gamma(r)/\gamma_o \rangle_{\gamma_o}, \tag{4}$$

where $\Gamma(r)$ is the value of the desired cluster integral or sum of integrals at a specific r, which is the relative distance between the root points. $\gamma(r)$ is the value of integrand or sum of integrands at r, the subscript "o" indicates a quantity for a reference system, for which Γ_o is assumed known. The angle bracket indicates an average over an ensemble of configurations. A key feature of free-energy methods is that they do not attempt direct evaluation of the free energy or configurational integral. Rather they deal with free-energy differences or integral ratios. Thus in Eq. (4) we calculate only the ratio of the target cluster integral(s) to a reference, and do not attempt direct evaluation of the cluster integral as is done in standard quadrature approaches.

Equation (4) is in fact the basic working formula for the methods of Rast *et al.* and Labík *et al.* To apply this formula, it is necessary that γ_0 be non-negative. This is easily accomplished by taking its absolute value, but one should recognize then that the definition of Γ_o must be modified accordingly. The application by Labík *et al.* uses a single cluster (framework) for γ_o, and considers only the hard-sphere potential, for which the cluster integrand has values 0 and +1 (or 0 and −1) only. Thus evaluation of Γ_o is not complicated by taking the absolute value of γ_o. Rast *et al.* do not restrict the choice of γ_o this way, and they use a more complicated form that depends on the absolute value of $h(r)$ between the sample points. They then applied a separate method involving unbiased sampling in an appropriate hypervolume to evaluate (the equivalent of) Γ_o.

A more flexible free-energy method is umbrella sampling, for which the working equation is as follows:

$$\Gamma(r) = \Gamma_o \frac{\langle \gamma(r)/\pi \rangle_\pi}{\langle \gamma_o/\pi \rangle_\pi}, \tag{5}$$

where π is a (non-negative) probability distribution that governs the sampling of all configurations of molecules. With this formulation we separate the reference cluster from its role as a sampling or bias function. This permits more leeway in its choice, so we can employ any cluster(s) in its definition, and it can be based on any intermolecular potential (not necessarily the one of interest). Regarding π, there is no specific restriction on its choice as long as it adequately samples all configurations important to both target and reference systems (therefore it is helpful to select γ_o so that its important configurations are similar to those for γ).

III. COMPUTATIONAL DETAILS

We define $\gamma(r)$ as the sum of the clusters defining a term $b_n(r)$ in the h-bond expansion of the bridge function. Values of $\Gamma(r)$ can be collected at different values of r in one simulation, by allowing the root points to sample separations freely. Thus contributions to the averages for $\gamma(r)$ are binned according to the value of r. Reported values of $\gamma(r)$ are

$$\gamma(r_i) = \frac{1}{V_i M} \sum_{k=1}^{m_i} \gamma_{i,k}, \tag{6}$$

where m_i is the number of times the root particles were observed to be separated by a distance in r_i to $r_i+\Delta r$, $\gamma_{i,k}$ is the kth contribution to the average in bin i, $M=\Sigma m_i$ is the total number of contributions made to all bins, and $V_i=\frac{4}{3}\pi[(r_i+\Delta r)^3-r_i^3]$ is the volume of the shell associated with bin i.

We choose the reference γ_o as a single ring cluster of field (no root) particles and with a number of particles the same as that appropriate to the bridge coefficient being calculated (including the root points). The bonds in γ_o are f bonds for a hard-sphere potential of unit diameter (which is the same diameter as the system of interest). Note that this cluster, and thus the denominator of Eq. (5) and also Γ_o, do not depend on r, so all configurations contribute to its average. For π we choose the absolute value of γ. The bias π also does not give any significance to the root points, and is not considered a function of r. This choice for π is certain to include all relevant configurations of γ, also, it is clear that the configurations important to γ_o are a subset of those important to γ and thus will be able to be sampled by this choice of π.

We also perform calculations in which the root points are held at a fixed separation. For these calculations γ_o is chosen as a chain of $|h|$ bonds (bonds defined as the absolute value of h), and π is chosen to be equal to γ_o. Thus we can calculate $\gamma(r)$ by averaging according to Eq. (4), with Γ_o a function of r. For this system $\Gamma_o(r)$ can be calculated from $|h(r)|$ using Fourier transform methods. Results calculated this way for several values of r were consistent with the calculations that permitted the root-point separations to fluctuate, and are not reported in detail here.

Equations (1) and (2) are solved in an incremental, iterative manner. We begin by evaluating the HNC solution $[b(r)=0]$ for $h(r)$ using the Picard iteration algorithm presented by Duh and Haymet.[33] The result is used to estimate $b(r)$ from its h-bond series expansion including only the b_2 term, which is evaluated by the Mayer-sampling technique using the HNC $h(r)$ interpolated from a table. This estimate of $b(r)$ is then used in another Duh–Haymet calculation of $h(r)$ via Eqs. (1) and (2), and this is used in a new Mayer-sampling calculation for $b_2(r)$. This b_2 is observed to differ little from the previous iteration, and is taken as the converged value. It is used in a corresponding process to calculate $b_3(r)$, alternating between solving for $h(r)$ and using the solution in Mayer-sampling calculations for b_3. We again perform a total of two Mayer-sampling calculations for this process, and then do the same for b_4, but do only one iteration so a single Mayer-sampling calculation is performed. In this scheme we do not revisit calculation of a b_n when higher-order coefficients are added to $b(r)$. All of these calculations are performed separately for densities from 0.1 to 0.9 in increments of 0.1 (where not otherwise specified, all values are given in units such that the hard-sphere diameter σ is unity).

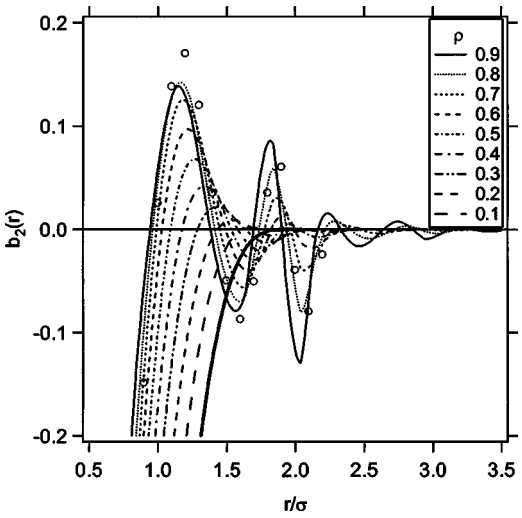

FIG. 2. Plot of bridge coefficient $b_2(r)$ with respect to the reduced distance. Different types of lines represent different densities ρ as shown in the legend. Open circles are results from Rast, Fries, and Krienke (Ref. 16) and bold line is the (density-independent) result of Labík *et al.* (Ref. 31).

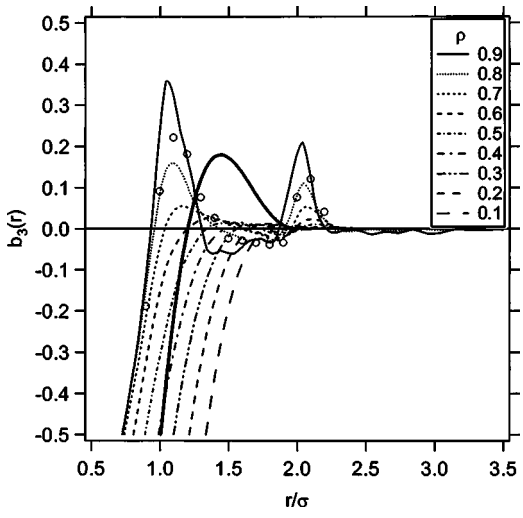

FIG. 3. Plot of bridge coefficient $b_3(r)$ with respect to the reduced distance. The same notation as in Fig. 2 is applied in this plot.

Tabulation of discretized $h(r)$ is performed up to separations of 10.24σ using 1024 bins, which makes $\Delta r = 0.01\sigma$. In many cases the tabulation can be performed to shorter separations, and so a cutoff distance is defined, beyond which $h(r)$ is taken to be zero. This cutoff was determined prior to the calculations by examining HNC values of the correlation function. Cutoff values of $h(r)$ are typically 3σ at density 0.1 and 8σ at 0.9. The bin size for tabulation of the bridge coefficients was much coarser, using a bin size $\Delta r = 0.1\sigma$. In simulations of the diagram for the second coefficient, the root points are found to go no further than 5σ apart; for the third coefficient, the observed maximum separation is about 6σ, and for the fourth coefficient, about 7σ is the largest separation. Note that the maximum separation for the distribution of bridge diagrams is much shorter than chain type cluster due to highly connected inner bonds of field-field and field-reference points. We apply Neville's algorithm[34] to interpolate between interval points of $b(r)$ and to extrapolate to outside of end points. This procedure is used to match up the number of bins of the bridge function with the correlation function for performing the next numerical iteration step. As described above, we perform two consecutive iterations to obtain final results, except evaluation of b_4 at densities 0.7, 0.8, and 0.9, where the MC Mayer-sampling simulations must typically collect $40-80\times10^9$ configurations to obtain the smooth results. For the other densities for b_4, we employ 10×10^9 configurations. For the coefficients b_2 and b_3, Mayer sampling yields good results with considerably less sampling; we used $1-2\times10^9$ samples in our calculations.

IV. RESULTS AND DISCUSSION

Figures 2 and 3 show results for $b_2(r)$ and $b_3(r)$, respectively, computed using the methods described above. At low densities, both functions appear smooth, but this behavior changes at higher density, where severe oscillations about zero are observed. A partial comparison with literature data is possible for the density 0.8, at which Rast, Fries, and Krienke[16] report data. Those results agree qualitatively with ours, but differ in a quantitative comparison. This discrepancy most likely originates from the use of different $h(r)$ in the cluster-integral calculations. Rast *et al.* use "exact" h bonds based on simulation data, while we use the incrementally self-consistent iterative approach detailed above. The failure to find complete agreement with a similar method based on exact h bonds uncovers a weakness in the approach we have employed.

We also evaluate $b_4(r)$ by the Mayer-sampling method, and show the results in Fig. 4. This calculation involved the evaluation of 56 clusters in the iterative scheme. There are no h-bond results from the literature available for comparison. At high densities, the confidence limits indicate large fluctuations, and this behavior becomes more serious as the relative distance of reference points gets smaller. We attempted to improve the confidence limits by applying additional sampling for this coefficient at these densities, using up to 80×10^9 configurations. The results are still less than

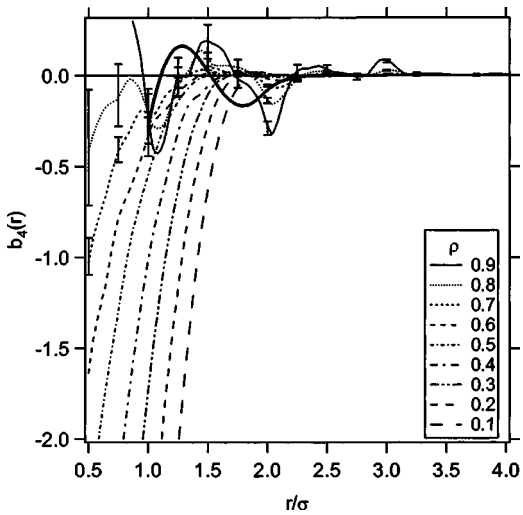

FIG. 4. Plot of bridge coefficient $b_4(r)$ with respect to the reduced distance. The same notation as in Fig. 2 is applied in this plot.

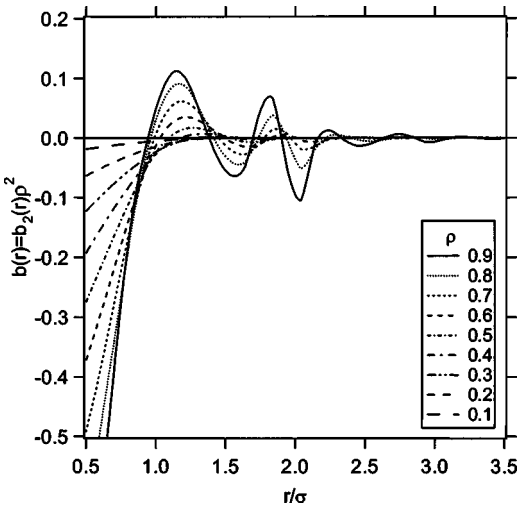

FIG. 5. Plot of bridge function $b(r)$ as given by the density expansion including only $b_2(r)$, with respect to the reduced distance. Different types of lines represent different densities as shown in the legend.

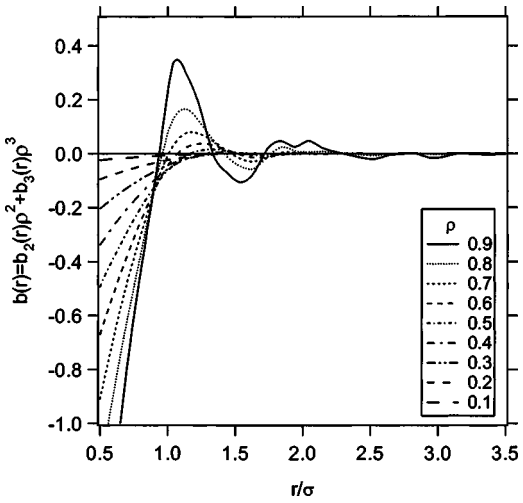

FIG. 6. Plot of bridge function $b(r)$ as given by the density expansion including $b_2(r)$ and $b_3(r)$, with respect to the reduced distance. Different types of lines represent different densities as shown in the legend.

satisfactory, and we speculate that a more effective approach to improve the results would involve a different Mayer-sampling strategy [other than Eq. (5)].

We also compare all our results to the f-bond cluster coefficients reported by Labík *et al.*,[31] who provided convenient empirical fits of their results. The f-bond clusters are density independent, so a single curve is given for each coefficient. It is clear from Fig. 2 that the Labík *et al.* result for the f-expansion $b_2(r)$ is a smooth extrapolation of our results in the limit $\rho \to 0$. Examination of Figs. 3 and 4 does not show the same connection. This is because some of the clusters in the f-bonded b_3 and b_4 are represented in the h-bonded b_2. Instead we find (not shown) that the sum $b_2 + b_3\rho$ with the f-bond coefficients is the $\rho \to 0$ limiting form of the same sum with the h-bond coefficients; a similar comparison applies using $b_2 + b_3\rho + b_4\rho^2$. The comparison also shows that the h-bond expansion does succeed in incorporating significantly more effects of density on $b(r)$ than the f-bond expansion is able.

Next we examine the bridge function itself as given using increasing orders of the density expansion. Figure 5 shows the bridge function composed of $b_2(r)$, Fig. 6 shows the bridge function containing $b_2(r)$ and $b_3(r)$, and Fig. 7 shows the bridge function determined with all three bridge coefficients measured here. We note that the present calculations show a non-negligible $b(r)$ to slightly larger separations than seen in the study by Rast, Fries, and Krienke.[16] Small effects in the long-range behavior of $b(r)$ can impact the pressure as computed by the compressibility formula, for which offsetting oscillations in $h(r)$ make an accurate determination difficult. We notice that the magnitude of bridge-function oscillations is not continuously increased as more coefficients are added to the expansion. The magnitude is rather reduced with the inclusion of the third coefficient. Figure 8 shows a comparison of our results to the literature determinations at density 0.8. Our results agree well with those by Rast, Fries, and Krienke[16] B_t (which includes b_2 only) but not with B_s (which includes b_2 and b_3). This can be explained again by the use of different $h(r)$ in the calculations. We also compare to two empirical formulas that aim to describe the true bridge function.[14,35] These equations are constructed with the assumption that the hard sphere $b(r)$ is nonpositive, and our results clearly disagree with them in this regard. Very careful studies performed recently to compute $b(r)$ from simulation data indicate now that the bridge function may take positive values, albeit of small magnitude (less than 0.01 for $\rho = 0.94$).[11] Inclusion of the third term in our results moves $b(r)$ toward the empirical formulas, but there remains a substantial difference between them.

We consider now the improvement of estimates of the radial distribution function $g(r)$ as higher-order terms in the bridge function are introduced to the HNC approximation. Figures 9 and 10 show different parts of $g(r)$ at density 0.8, compared with results of molecular dynamics simulation performed by us. Contact values of $g(r)$ (Fig. 9) decrease toward the simulation result as the bridge function includes more bridge coefficients, while the improvement around the second peak is not so clear (Fig. 10). Regardless, the rate of

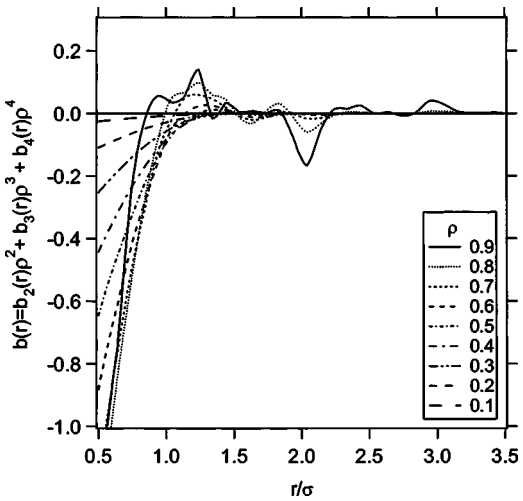

FIG. 7. Plot of bridge function $b(r)$ as given by the density expansion including $b_2(r)$, $b_3(r)$, and $b_4(r)$, with respect to the reduced distance. Different types of lines represent different densities as shown in the legend.

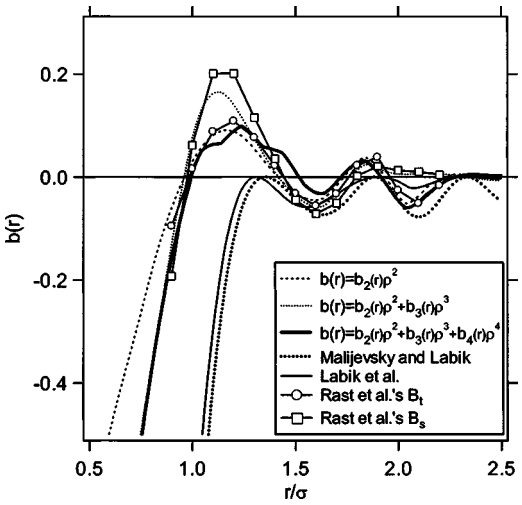

FIG. 8. Plot of bridge function $b(r)$ with respect to the reduced distance at reduced density $\rho\sigma^3=0.8$. Bold dotted line represents the parametrized bridge function of Malijevsky and Labík (Ref. 14) Solid line without markers describes the Verlet-modified bridge function, which is determined by Labík, Malijevsky, and Smith (Ref. 35). Lines with symbols are data from the *h*-bond cluster study of Rast, Fries, and Krienke (Ref. 16) for which B_t is $b_2(r)\rho^2$ and B_s is $b_2(r)\rho^2+b_3(r)\rho^3$.

convergence is not very high, and it appears that to obtain good contact values at the high density region at least several more coefficients would be needed in the bridge function. This involves a very large number of clusters, and is likely to be beyond the limits of what can be feasibly calculated even with Mayer-sampling methods.

Finally, we examine the pressure as a function of density, calculated using both the compressibility and virial routes, using the total correlation function $h(r)$ determined with each level of truncation of the bridge-function series. Figure 11 shows our results compared to the accurate Carnahan–Starling equation of state.[36] As is well known, for hard spheres the virial pressure determined by pure HNC overestimates the true pressure and the PY virial underestimates it, while the opposite holds for the pressure computed via the compressibility equation. As higher-order terms in the bridge-function expansion are added, results from this study show gradual improvement over the entire range of density. The improvement is more significant for the pressure as computed via the virial, though even with the highest-order treatment the modified HNC barely improves upon the PY compressibility result. The modified HNC pressure computed via the compressibility has very large error bars at the higher densities, and does not provide useful results. Again, it seems that several more coefficients would be needed to obtain good contact values at even moderate densities.

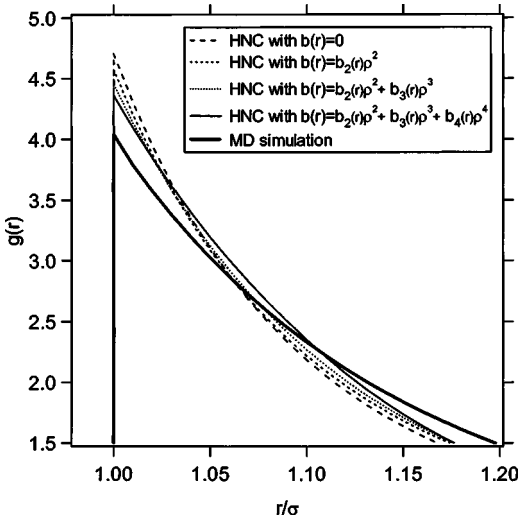

FIG. 9. Plot of $g(r)$ at density 0.8 at separations near contact value. Bold line is our result of molecular dynamics simulations [based on simulating 1372 particles after discarding about 10^6 collisions and collecting an average $g(r)$ for about 10^8 collisions]; other lines (marked "HNC with…") are from solution of the Ornstein–Zernike equation with a bridge-function closure obtained from the *h*-bond cluster expansion to the indicated order in density.

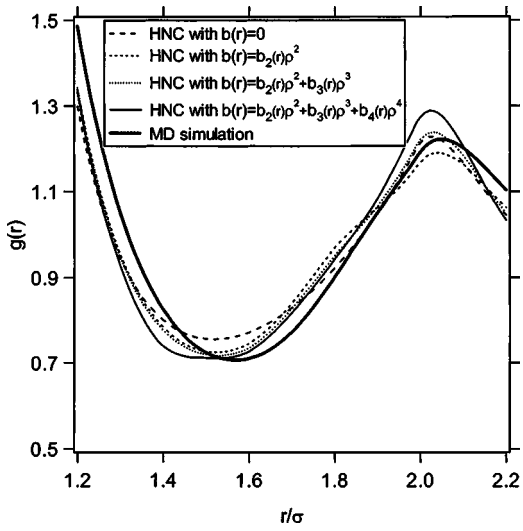

FIG. 10. Same as Fig. 9, but expanding on the region near the second peak in $g(r)$.

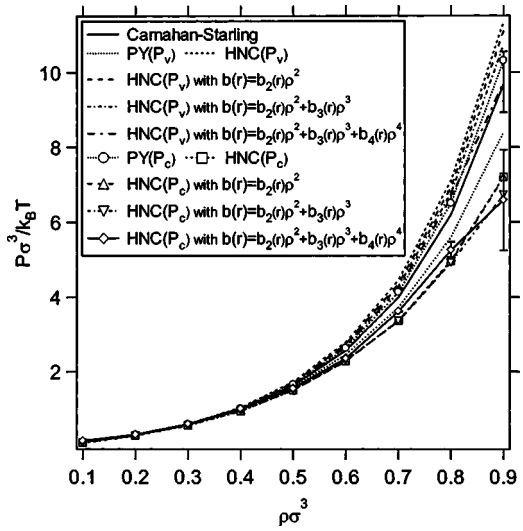

FIG. 11. Plot of pressure with respect to the reduced density. Solid line is the semiempirical equation of state of Carnahan and Starling (Ref. 36). Lines marked PY are from the Percus–Yevick theory, and lines marked "HNC with…" are from solution of the Ornstein–Zernike equation with a bridge-function closure obtained from the *h*-bond cluster expansion to the indicated order in density. Subscripts "v" and "c" indicate the pressure obtained from the correlation function via the virial and compressibility equations, respectively. Error bars are included only when significant, and are visible only on the HNC+fourth-order bridge function expansion, at densities greater than 0.7.

V. CONCLUSION

In this study, we demonstrated the Mayer-sampling method for evaluation of cluster integrals as applied to calculation of clusters having two root points (and thus a function of the separation of two particles). The method has been applied previously only to clusters relevant to the virial coefficients, and which have just one root point, so this represents a useful extension of the method.

We performed calculations for the coefficients of the h-bond series of the bridge function, applied to the hard-sphere model system. The procedure requires some iteration, as the h function itself is being determined in the procedure. The h-bond clusters have been computed in previous work, but they employed data for $h(r)$ determined by independent means. Also, the previous work treated only clusters to order ρ^3, while in the present work we computed clusters up to the next higher order in density. The present work provides a demonstration of how the h-bond clusters can be computed iteratively with the determination of $h(r)$ itself. We find that our results differ slightly from previously calculated h-bond clusters (where comparison is possible), and we attribute this to the different $h(r)$ used in the calculations. We expect that we could find improvement if we did not use an incremental process, and instead used the $h(r)$ determined considering higher-order coefficients of $b(r)$ to feed back into the calculation of the lower-order coefficients. Alternatively we could perform the iterative calculation of $h(r)$ considering all the bridge coefficients (up to a specified order) at once.

At low densities, the calculated hard-sphere bridge function is nonpositive, but at higher densities oscillations are seen, with the approximate bridge function taking positive values. So far, even with addition of the third coefficient, comparison with simulation data for the structure and thermodynamic properties indicates that the accuracy of the approximate bridge function is not high. Calculation of the fourth bridge coefficient involves 1731 distinct diagrams, and the number of clusters in higher-order coefficients exponentially increases. We think that evaluation of an additional term or two is feasible using the methods described here, but the slow rate of convergence seems to make the effort not worthwhile, at least for this hard-sphere application. Our approach to obtain $b(r)$ can be applied to any model systems with relatively simple modifications. Extensions or other applications may wish to consider other Mayer-sampling approaches, which might yield results of better quality more efficiently.

ACKNOWLEDGMENTS

This work was supported by the Division of Chemical Sciences, Office of Basic Energy Sciences of the U.S. Department of Energy (Contract No. DE-FG02-96ER14677), and by the U.S. National Science Foundation (Grant No. CTS-0414439). Computer resources were provided by the University at Buffalo Center for Computational Research. We are grateful to Peter Monson for computer codes that assisted with the integral-equation calculations.

[1] J. P. Hansen and I. R. McDonald, *Theory of Simple Liquids*, 2nd ed. (Academic, London, 1986).
[2] C. Caccamo, Phys. Rep. **274**, 1 (1996).
[3] P. Hutchinson and W. R. Conkie, Mol. Phys. **21**, 881 (1971).
[4] D. S. Hall and W. R. Conkie, Mol. Phys. **40**, 907 (1980).
[5] G. A. Martynov and G. N. Sarkisov, Mol. Phys. **49**, 1495 (1983).
[6] F. J. Rogers and D. A. Young, Phys. Rev. A **30**, 999 (1984).
[7] P. Ballone, G. Pasore, G. Galli, and D. Gazzillo, Mol. Phys. **59**, 275 (1986).
[8] A. G. Vompe and G. A. Martynov, J. Chem. Phys. **100**, 5249 (1994).
[9] Y. Rosenfeld, Phys. Rev. E **54**, 2827 (1996).
[10] R. Fantoni and G. Pastore, J. Chem. Phys. **119**, 3810 (2003).
[11] J. Kolafa, S. Labik, and A. Malijevsky, Mol. Phys. **100**, 2629 (2002).
[12] L. Verlet and J. J. Weis, Phys. Rev. A **5**, 939 (1972).
[13] D. Henderson and E. W. Grundke, J. Chem. Phys. **63**, 601 (1975).
[14] A. Malijevsky and S. Labik, Mol. Phys. **60**, 663 (1987).
[15] S. B. Yuste and A. Santos, Phys. Rev. A **43**, 5418 (1991).
[16] S. Rast, P. H. Fries, and H. Krienke, Mol. Phys. **96**, 1543 (1999).
[17] E. Meeron and A. J. F. Siegert, J. Chem. Phys. **48**, 3139 (1968).
[18] E. W. Grundke and D. Henderson, Mol. Phys. **24**, 269 (1972).
[19] S. Labik and A. Malijevsky, Mol. Phys. **67**, 431 (1989).
[20] L. L. Lee, J. Chem. Phys. **103**, 9388 (1995).
[21] L. L. Lee, J. Chem. Phys. **110**, 7589 (1999).
[22] F. Lado, Phys. Rev. **135**, 1013 (1964).
[23] F. Lado, Phys. Rev. A **8**, 2548 (1973).
[24] Y. Rosenfeld and N. W. Ashcroft, Phys. Rev. A **20**, 1208 (1979).
[25] F. Lado, S. M. Foiles, and N. W. Ashcroft, Phys. Rev. A **28**, 2374 (1983).
[26] G. Stell, in *The Equilibrium Theory of Classical Fluids*, edited by H. L. Frisch and J. L. Lebowitz (Benjamin, New York, 1964), p. 11170.
[27] B. R. A. Nijboer and L. van Hove, Phys. Rev. **85**, 777 (1952).
[28] Y. T. Lee, F. H. Ree, and T. Ree, J. Chem. Phys. **26**, 3506 (1968).
[29] P. Attard and G. N. Patey, J. Chem. Phys. **92**, 4970 (1990).
[30] J. S. Perkyns, K. M. Dyer, and B. M. Pettitt, J. Chem. Phys. **116**, 9404 (2002).
[31] S. Labik, H. Gabrielova, J. Kolafa, and A. Malijevsky, Mol. Phys. **101**, 1139 (2003).
[32] J. K. Singh and D. A. Kofke, Phys. Rev. Lett. **92**, 220601 (2004).
[33] D.-M. Duh and A. D. J. Haymet, J. Chem. Phys. **103**, 2625 (1995).
[34] W. H. Press, S. A. Teukolsky, W. T. Vetterling, and B. P. Flannery, *Numerical Recipes: The Art of Scientific Computing*, 2nd ed. (Cambridge University Press, Cambridge, 1992).
[35] S. Labik, A. Malijevsky, and W. R. Smith, Mol. Phys. **73**, 87 (1991).
[36] N. F. Carnahan and K. E. Starling, J. Chem. Phys. **51**, 635 (1969).